

# Time-resolved observations of vibrationally excited NO X $^2\Pi$ ( $\nu'$ ) formed from collisional quenching of NO A $^2\Sigma^+$ ( $\nu = 0$ ) by NO X $^2\Pi$ : evidence for the participation of the NO a $^4\Pi$ state.

James D. Fletcher,<sup>a</sup> Lucia Lanfri,<sup>b</sup> Grant A.D. Ritchie<sup>\*a</sup> Gus Hancock,<sup>a</sup> Meez Islam<sup>c</sup> and Graham Richmond.<sup>a</sup>

<sup>a</sup>Department of Chemistry, Oxford University, Physical and Theoretical Chemistry Laboratory, South Parks Road, Oxford OX1 3QZ, UK.

<sup>b</sup>Universidad Nacional de Córdoba, INFIQC CONICET, Córdoba, Argentina.

<sup>c</sup>School of Science and Engineering, Teesside University, Middlesbrough, TS1 3BA, UK.

E-mail: [grant.ritchie@chem.ox.ac.uk](mailto:grant.ritchie@chem.ox.ac.uk)

## Abstract

Time-resolved observations have been made of the formation of vibrationally excited NO X  $^2\Pi$  ( $\nu'$ ) following collisional quenching of NO A  $^2\Sigma^+$  ( $\nu = 0$ ) by NO X  $^2\Pi$  ( $\nu = 0$ ). Two time scales are observed, namely a fast production rate consistent with direct formation from the quenching of the electronically excited NO A state, together with a slow component, the magnitude and rate of formation of which depend upon NO pressure. A reservoir state formed by quenching of NO A  $^2\Sigma^+$  ( $\nu = 0$ ) is invoked to explain the observations, and the available evidence points to this state being the first electronically excited state of NO, a  $^4\Pi$ . The rate constant for quenching of the a  $^4\Pi$  state to levels  $\nu' = 11 - 16$  by NO is measured as  $(8.80 \pm 1.1) \times 10^{-11} \text{ cm}^3 \text{ molecule}^{-1} \text{ s}^{-1}$  at 298 K where the error quoted is two standard deviations, and from measurements of the increased formation of high vibrational levels of NO(X) by the slow process we estimate a lower limit for the fraction of self-quenching collisions of NO A  $^2\Sigma^+$  ( $\nu = 0$ ) which lead to NO a  $^4\Pi$  as 19%.

## Introduction

The first electronically excited state of NO, a  $^4\Pi$ , lies some 4.75 eV above the ground X  $^2\Pi$  state,<sup>1,2</sup> and both of these states correlate with the separated atoms in their ground N ( $^4S$ ) and O ( $^3P$ ) states.<sup>3,4</sup> The afterglows associated with the recombination of the atoms is believed to take place largely through initial formation of the a  $^4\Pi$  state, which then undergoes a variety of processes leading to electronically excited states from which spin-allowed optical transitions can be observed, namely the A  $^2\Sigma^+$ , b  $^4\Sigma^-$ , B  $^2\Pi$  and C  $^2\Pi$  states giving rise to the  $\gamma$ , Ogawa,  $\beta$  and  $\delta$  bands respectively.<sup>3-6</sup> The identification of “gateway states” through which population can flow between the a and B states has allowed high resolution measurements of the Ogawa bands to be combined with those of the  $\beta$  bands to determine the relative energy levels of the quartet and doublet manifolds.<sup>1,2,7,8</sup>

Despite the importance of the a  $^4\Pi$  state, very little is known about its gas-phase kinetic behaviour, largely because of the difficulty in preparing and detecting it in a sensitive quantum state-resolved fashion. Direct excitation in the spin forbidden (and weak) a – X transition has been achieved for high vibrational levels ( $v = 11 - 15$ ), where the Franck Condon factors maximise, with detection being either through emission from the gateway levels in the B state<sup>8-10</sup> or by surface ionisation of the metastable a  $^4\Pi$  state produced in a molecular beam.<sup>2</sup> The former method has been used to determine collisional removal rates of NO a  $^4\Pi$  ( $v = 11$ ) with NO, O<sub>2</sub>, N<sub>2</sub>O, N<sub>2</sub>, CO<sub>2</sub>, He and Ar.<sup>9-11</sup> The reverse processes (removal of the approximately energetically equivalent vibrational levels of the B state) have also been reported, with the conclusion that these processes are fast, with rate constants ranging from  $10^{-12}$  to  $10^{-10}$  cm<sup>3</sup> molecule<sup>-1</sup> s<sup>-1</sup>.<sup>10,11</sup> One measurement has been reported which is pertinent to levels below  $v = 11$ : Ottinger and Shen<sup>12</sup> used a molecular beam technique to form vibrationally excited NO a  $^4\Pi$ , collided it with ground state NO and observed  $\gamma$  band emission resulting from formation of NO A  $^2\Sigma^+$  in the process:



From a comparison of the  $\gamma$  band emission intensity with that from a similar energy exchange process involving N<sub>2</sub> A  $^3\Sigma_u^+$  they deduced that the cross section for process (1) with NO a  $^4\Pi$  in vibrational levels  $v \geq 6$  (the energy requirement for formation of NO A  $^2\Sigma^+$  ( $v = 0$ )) was 2 Å<sup>2</sup>.

The A  $^2\Sigma^+$  state of NO lies some 5.47 eV above the ground state,<sup>13</sup> and the a  $^4\Pi$  and X  $^2\Pi$  states are the only ones lying below it in energy (the next highest state, B  $^2\Pi$ , lies 0.162 eV above the A state). The inelastic collisional quenching of NO A  $^2\Sigma^+$  ( $v = 0$ ) by NO X  $^2\Pi$  ( $v = 0$ ) at room temperature can thus only form the a and X states on energetic grounds. Despite the enormous amount of effort that has been expended on the determination of the rates of quenching of the A state (mainly because of the importance of laser induced fluorescence (LIF) of the A – X transition as a detection method for NO in combustion and aeronomy), very little is known about the quantum states of the products, and inelastic

energy transfer studies have been confined to quantum state distributions in the ground  $X^2\Pi$  state. Settersten *et al.* determined the fraction of  $NO\ A^2\Sigma^+ (v=0)$  returned to the ground state  $X^2\Pi (v'=0)$  in collisions with  $O_2$ ,  $CO$ ,  $CO_2$  and  $H_2O$ , showing remarkably high values (60% for  $CO_2$ , 30% for the other gases).<sup>14</sup> We have used the technique of time-resolved FTIR emission (TRFTIRE) spectroscopy to determine the quantum state distributions in  $NO\ X^2\Pi (v')$  for the inelastic energy transfer channels for quenching of  $NO\ A^2\Sigma^+ (v=0)$  in collisions with  $NO\ X^2\Pi$ ,<sup>15</sup>  $CO_2$ ,<sup>16</sup>  $N_2O$ <sup>16</sup> and  $O_2$ .<sup>17</sup> TRFTIRE showed considerable vibrational excitation in the ground state  $NO\ X^2\Pi (v')$  product, but detectable vibrational emission from levels of the  $NO\ a^4\Pi$  state would not be expected in these experiments: the fundamental vibrational emission bands of  $NO\ a^4\Pi$  lie below  $1000\ cm^{-1}$ , outside the range of the detector used. The overtone bands lie in detectable regions, but considerations of their band positions and emission intensities<sup>18</sup> indicate that they would be overlapped by stronger fundamental and overtone emission bands from the  $NO\ X^2\Pi$  state vibrational levels formed by quenching.

In this paper we describe further studies of the infrared emission observed from  $NO\ X^2\Pi (v')$  when  $NO\ A^2\Sigma^+ (v=0)$  is formed by excitation at 226 nm and removed by both fluorescence in the  $A-X$  band and by self-quenching. Here we use a HgCdTe detector of rise time 200 ns, over a factor of 10 faster than the InSb detector used previously, and this has resulted in the observation of two time scales for the formation of high vibrational levels of  $NO\ X^2\Pi (v')$ . We observe a fast component on the time scale expected as a result of direct  $A-X$  quenching (dominated by the radiative lifetime of  $NO\ A^2\Sigma^+ (v=0)$ , 192.6 ns<sup>19</sup>) together with an indirect component, the rate and magnitude of which is dependent on NO pressure. We propose that this emission is evidence that self-quenching of  $NO\ A^2\Sigma^+ (v=0)$  produces non-negligible population in the elusive  $a^4\Pi$  state, which is then quenched by NO to the ground electronic state. We have estimated a lower limit of 19% for the fraction of self-quenching collisions which lead to the formation of  $NO\ a^4\Pi$ .

## Experimental

The TRFTIRE experimental setup has been described in detail in previous articles,<sup>15,20-22</sup> therefore only a brief overview is provided in this section.  $NO\ A^2\Sigma^+ (v=0)$  is produced by the excitation of ground state  $X^2\Pi (v'=0)$  nitric oxide with radiation of wavelength 226.26 nm, which is tuned to the overlapped  $Q_1$  and  $Q_{21}$  band heads of the  $A^2\Sigma^+ \leftarrow X^2\Pi (0,0)$  transition. Static samples of NO and Ar were introduced into a stainless steel vacuum chamber evacuated by a turbomolecular pump (Leybold Turbo Vac 340M). The chamber was equipped with multi-pass mirrors to propagate the UV excitation pulses. IR radiation emitted by vibrationally excited products was directed out of the chamber by a Welsh Cell optical arrangement through a  $CaF_2$  window.<sup>23</sup> Upon exiting the chamber through the window, the collected emission was directed into a FTIR spectrometer (Bruker IFS66s) operating in step-scan mode and using a fast HgCdTe detector (Vigo PVI-4TE) sensitive from 2.5 to 4.0  $\mu m$ . IR

emission was averaged for typically 30 laser shots for each mirror position within the spectrometer and normalised to the intensity of the LIF produced by radiative decay of NO  $A^2\Sigma^+$  ( $v = 0$ ), the intensity of which is directly proportional to the number of excited state molecules produced following interaction with the laser pulse, thus accounting for small variations in laser output power during the data acquisition. The interferograms produced by step-scanning the interferometer underwent Fourier Transform to yield time-resolved emission spectra. The fast detector is noisier than the slower InSb detector used previously<sup>15,20-22</sup> and 10 spectra were co-added to improve S/N ratios.

In other experiments the FTIR spectrometer was bypassed and emission exiting the chamber was focused onto the detector using a CaF<sub>2</sub> lens, with optical filters used to transmit selected wavelengths of NO emission corresponding to specific ranges of vibrational levels within the X state. This resulted in more efficient collection of IR emission from the reaction chamber and allowed a rapid comparison of IR emission signals from specific vibrational levels under different conditions. The time response of the detector/encapsulated amplifier combination was measured from its response to a 10 ns laser pulse. The rise time (10 – 90%) was found to be *ca.* 200 ns, but an electronic ringing (described later) affected the data between 0.5 – 1.5  $\mu$ s. NO was prepared from a commercial sample (purity > 99.5 %, BOC) by freezing out contaminants (principally NO<sub>2</sub>) using an ethanol slush bath. Ar (BOC 99.998%) was used without further purification. All experiments were carried out at room temperature (295 K).

## Results

### A. TRFTIRE from NO X $^2\Pi$ ( $v'$ )

Figure 1 shows the FTIR emission spectra in the region corresponding to first overtone transitions ( $\Delta v' = -2$ ) within NO X  $^2\Pi$  observed at two times following the excitation of 100 mTorr NO in 50 Torr Ar at 226.26 nm. Ar was added to increase the signal levels through rotational hole filling, and to ensure rotational (but not vibrational) thermalisation of the products.<sup>15</sup> First overtone transitions within NO X  $^2\Pi$  lead to constructive interference of overlapping P and R branches of the rotationally thermalized vibrational transitions and yield structured emission spectra as in Figure 1, even at relatively low resolution, as described in detail in previous publications.<sup>15-17, 20-22</sup> Band origins are marked on the figure showing populations up to  $v' = 20$ . The effect of Ar was shown to make negligible changes to the spectrum, other than a slight diminution of the populations in higher levels caused by vibrational relaxation at Ar pressures above 200 Torr, consistent with the known slow rates of electronic quenching of NO  $A^2\Sigma^+$  ( $v = 0$ )<sup>24</sup> and vibrational relaxation of NO X  $^2\Pi$  ( $v'$ ).<sup>22</sup>

Two spectra are shown on the same relative scale, summing the signals over 1  $\mu$ s time intervals at “early” and “late” times, namely from 0.8 – 1.8  $\mu$ s and from 9 – 10  $\mu$ s, illustrating that there is a marked difference between them. Signals from low  $v'$  (above 3600 cm<sup>-1</sup>, the (4,2) band origin) are virtually unchanged, whereas in the high  $v'$  region an increase is seen at later times with the largest

change being approximately a factor of two near  $3200\text{ cm}^{-1}$ , a region corresponding to emission from  $v' = 11$  and  $12$ . The time intervals were chosen to illustrate this difference in the following way. By  $0.8\text{ }\mu\text{s}$  we expect population of  $\text{NO } X^2\Pi(v')$  from electronic quenching of  $\text{NO } A^2\Sigma^+(v=0)$  to be complete, as the combination of radiative<sup>19</sup> and collisional<sup>25</sup> decay rates yield a lifetime of  $164\text{ ns}$  at  $100\text{ mTorr}$   $\text{NO}$ , and the signal levels should be largely unaffected by the  $200\text{ ns}$  detector rise time. Between  $9$  and  $10\text{ }\mu\text{s}$  there will be some population decrease by vibrational relaxation, but this will only be noticeable in the lowest and highest levels that we observe: the self-relaxation rate constants give a relaxation lifetime at  $100\text{ mTorr}$  of *ca.*  $100\text{ }\mu\text{s}$  for  $v' = 2$ ,<sup>22,26-29</sup> they show a minimum at  $v' = 9$ <sup>22</sup> and increase at high  $v'$ ,<sup>22,30</sup> giving a lifetime of  $30\text{ }\mu\text{s}$  at the highest level probed,  $v' = 20$ .<sup>30</sup> The infrared signals after  $1\text{ }\mu\text{s}$  rise with a time constant of *ca.*  $4\text{ }\mu\text{s}$ , reach a plateau and show wavelength dependent decays at longer times consistent with vibrational energy loss by self-relaxation. A repeat of the TRFTIRE experiment with  $200\text{ mTorr}$   $\text{NO}$  showed similar increases in signals from high vibrational levels, with the time taken to reach the plateau halving, and the long-time decay rates doubling. It appears that a collisional process involving  $\text{NO}$  causes the slower process.

## B. Filter experiments

Six infrared optical filters a) – f) were used, with the centres of their transmission bands marked in Figure 1. Initial experiments involved excitation of  $50\text{ mTorr}$   $\text{NO}$  at  $226\text{ nm}$ , with  $8\text{ Torr}$   $\text{Ar}$  present. The  $\text{Ar}$  pressure ensured that diffusion of the emitting species out of the detected volume was prevented, that rotational hole filling augmented the signal levels, yet was not sufficient to compromise the longer time signals through vibrational relaxation. Emission traces obtained for filters a) – f) are shown in Figure 2. We note the following behaviour. Firstly, in trace a) (emission from  $v' = 2 - 4$ ) we see that the signal rises rapidly after the laser pulse (within a few hundred ns), showing an unavoidable electronic ringing as a result of the encapsulated amplifier electronics. Apart from the ringing the signal clearly consists of only one rising component. Traces with filters b) – f) exhibit a similar rapid rise after the laser pulse but also display an additional component which rises on a much slower time scale with magnitudes relative to those of the rapid rise which are filter and hence vibrational level dependent. The relative magnitudes of the fast and slow signals for the different spectral regions are in agreement with the qualitative conclusions reached from the spectra shown in Figure 1 – no slow component observable at low  $v'$  (filter a)), a ratio of approximately unity for the fast and slow processes near  $3396\text{ cm}^{-1}$  (filter e) observing levels  $v' = 13 - 16$ ) and  $3160\text{ cm}^{-1}$  (filter d) observing levels  $v' = 11 - 13$ ), and a dominance of the fast over the slow process for filters b) (observing levels  $v' = 5 - 7$ ), c) (observing levels  $v' = 7 - 9$ ) and f) (observing levels  $v' = 17 - 20$ ).

Additional experiments were carried out to determine the mechanism for forming vibrationally excited NO(X). Identical excitation spectra were observed when either LIF or IR emission was monitored as a function of uv wavelength near 226 nm, clearly indicating that A state excitation is required to produce the IR emission. As previously<sup>15</sup> the excitation spectra showed enhancement of weaker branch lines in comparison with calculated non-saturated spectra, and this was expected<sup>31</sup> at the fluences which were needed in these experiments to achieve a usable S/N ratio for the IR emission (between 5 and 20 mJ cm<sup>-2</sup>). LIF signals were measured for laser fluences between 130  $\mu$ J cm<sup>-2</sup> and the maximum of 20 mJ cm<sup>-2</sup>, and showed a monotonic increase in intensity which deviated from linearity at the higher values, indicating partial saturation. IR emission could only be measured over the range 2 - 20 mJ cm<sup>-2</sup>, and showed a linear relationship with LIF intensity at constant NO pressure, again consistent with a common origin for LIF and IR emission (and justifying the normalisation of the IR signals with variation of the 226 nm laser output). Furthermore both the time dependences of the IR signals and the ratio between fast and slow components' magnitudes were invariant with laser fluence, behaviour which would not be expected if substantial sequential excitation of NO via the A state was occurring, unless the second transition was saturated at all fluences. This evidence also rules out the formation of the emitting levels by collisions between two vibrationally excited NO X <sup>2</sup>II ( $\nu'$ ) species. At 226 nm sequential excitation from the A state is known to produce ionisation, and from the measured ionisation cross section ( $7 \times 10^{-19}$  cm<sup>2</sup> <sup>32</sup>) we calculate that some 1.6% of the A state will be ionised at the maximum fluence used. Electrons have been shown (by addition of an electron scavenger<sup>15</sup>) to play no role in the IR emission: ion yields increase faster than linearly at laser fluences near 20 mJ cm<sup>-2</sup>,<sup>31</sup> and thus our measured fluence dependences are inconsistent with further involvement of this low fraction of ions in the IR emission. All the available evidence is consistent with the IR emission originating from both fluorescence and collisional processes involving the NO A <sup>2</sup> $\Sigma^+$  ( $\nu = 0$ ) level.

We next show how the rate of the slow indirect process depends upon the concentration of NO, [NO]. The absolute magnitudes of all the traces increased with [NO], as more parent molecules are excited at higher pressures. To attempt to compensate for this we normalise the signals to the UV fluorescence intensity as described above, and Figure 3 shows normalised data for three filter regions (a), d) and e)) at pressures of NO between 20 and 100 mTorr, in each case with 8 Torr Ar. Providing the uv normalisation method is robust, the relative magnitudes of the signals for a given filter are representative of the behaviour of a constant concentration of NO A <sup>2</sup> $\Sigma^+$ . For filter a) we now see a slow pressure dependent decay accompanying the fast process, with a slight decrease in the magnitude of the fast process with increasing [NO]. This is consistent with the formation of these low vibrational levels dominantly by fluorescence, with the decrease partially resulting from a slight lowering of the fraction of emission from NO X <sup>2</sup>II ( $\nu'$ ) levels formed by fluorescence and transmitted by filter a). Such fractions can be calculated from our previous values of the  $\nu'$  level populations produced by quenching of and fluorescence from the A state,<sup>15</sup> and change from 98% at 20 mTorr to 90% at 100 mTorr. The slow loss

is from vibrational relaxation. For filters d) and e) the fraction of emission caused by fluorescence population of the levels passed by the filters is far lower: a similar calculation puts this fraction less than 3%. Now, the amplitudes of both the initial fast process and the slow indirect process are seen to increase with pressure of NO, with the rate of the slow process also increasing. A slow decay is seen, more evident with the higher vibrational level filter e), and again is consistent with vibrational self-relaxation.

In the absence of any multiple excitation processes, the only potential candidates for the reservoir state leading to collisional population of the observed vibrational levels after the NO A  $^2\Sigma^+$  state has relaxed (the slow process) are either very high vibrational levels of the X  $^2\Pi$  state (higher vibrational levels than those seen in Figure 1) or the lowest excited electronic state, a  $^4\Pi$ . We shall show later that the reservoir state is produced with a quantum yield  $\geq 19\%$  from self-quenching of NO A  $^2\Sigma^+$ . If highly vibrationally excited NO X  $^2\Pi$  is the reservoir, then we should expect emission from such high levels, red shifted from the emission seen in Figure 1 and decaying with a time constant similar to that seen for the rise of the slow component of filters d) and e). The  $v = 0$  level of the A state is approximately isoenergetic with  $v' = 30$  in the ground state, and we would expect emission in the (30, 28) band at *ca.* 2160  $\text{cm}^{-1}$ . Einstein A factors have been calculated for  $\Delta v' = -2$  transitions within the X  $^2\Pi$  state for upper vibrational quantum numbers up to  $v' = 28$ .<sup>33</sup> The values maximise for the (27, 25) band, and show a minimal (less than 1%) decrease for  $v' = 28$ . We may estimate the magnitude of such emission in comparison with that seen from a high level of NO ( $v' = 19$ ) at 2750  $\text{cm}^{-1}$  in Figure 1, for which we know the relative quantum yield of collisional production, 0.5%.<sup>15</sup> If 19% quenching of the A state led to exclusive production of  $v' = 30$  and if the Einstein A coefficient for the (30, 28) band was assumed to be 10% smaller than that calculated for the (28, 26) band, then emission near 2160  $\text{cm}^{-1}$  would be expected to be a factor of 43 larger than at 2760  $\text{cm}^{-1}$ . In the many spectra that we have taken we see no such emission from these very high levels. We are led to the conclusion that high vibrational levels of NO X  $^2\Pi$  ( $v'$ ) cannot be the reservoir state, and thus the NO a  $^4\Pi$  state is involved. Collisional and radiative processes from the NO A  $^2\Sigma^+$  state produce NO X  $^2\Pi$  and yield the early time spectrum shown in Figure 1: A  $^2\Sigma^+$  state collisional quenching also produces NO a  $^4\Pi$  which undergoes collisions with ground state NO X  $^2\Pi$  ( $v' = 0$ ) to form the additional levels resulting in the extra components seen in the late time spectrum of Figure 1.

### C. Kinetic analysis – rate constants

We now analyse the data of Figs 2 and 3 with the following kinetic scheme. The decay of the A state will be single exponential with a rate equal to the sum of the total fluorescence (A – X) and collisional (A – X and A – a) rates. The fluorescence rate constant, which we call  $k_F$ , is given by the inverse of the A state radiative lifetime, 192.6 ns.<sup>19</sup> The collisional quenching rate constant of the A state with NO ( $2.71 \times 10^{-10} \text{ cm}^3 \text{ molecule}^{-1} \text{ s}^{-1}$ )<sup>25</sup> is measured as a total collisional loss, and is thus the sum of the rate constants which lead to the X and a states,  $k_{AX} + k_{Aa}$ . The total rate of loss of the A state, given by the sum of the radiative and collisional processes, ranges from  $5.37 \times 10^6 \text{ s}^{-1}$  at 20 mTorr to  $6.05 \times 10^6 \text{ s}^{-1}$  at 100 mTorr, *i.e.* it is dominated by the radiative term over the pressure range used in Figure 3. We call the pseudo first order rate constant for loss of the A state  $k_A$ , where  $k_A = k_F + (k_{AX} + k_{Aa})[\text{NO}]$ . NO a  $^4\Pi$  will be formed with a time dependence which reflects this radiatively dominated value, and we assume initially that formation results in the population of a single vibrational state  $v$  with a rate constant  $k_{Aa}$ . Loss of population from the a  $^4\Pi$  state occurs purely by collisions with NO to form the X state, as the a – X radiative rate is negligible,<sup>34</sup> and we call the overall bimolecular rate constant  $k_{aX}$ . Figure 4 shows the kinetic scheme for population of a specific vibrational level  $v'$  in the X state, with the rates for each process controlled by the overall rate constants  $k_F$ ,  $k_{AX}$  and  $k_{aX}$  multiplied by their quantum yields into level  $v'$ , namely  $\Phi_F^{v'}$ ,  $\Phi_{AX}^{v'}$  and  $\Phi_{aX}^{v'}$ . The rate constant  $k_{V,v'}$  is the bimolecular rate constant for net removal of the vibrational level  $v'$  in collisions with NO. The kinetic scheme can be solved explicitly to yield the time dependence of each NO X  $^2\Pi(v')$  level:

$$[\text{NO X}^2\Pi(v')](t) = Ae^{-k_{V,v'}[\text{NO}]t} - Be^{-k_A t} - Ce^{-k_{aX}[\text{NO}]t} \quad (2)$$

Here the coefficients  $A$ ,  $B$  and  $C$  are functions of the specific rate constants into and out of the vibrational level  $v'$  and expressions for these are given in the Appendix. The values of  $k_{V,v'}$  will depend on the vibrational relaxation rate constants both into and out of the level  $v'$  and should therefore be smaller than the specific one quantum loss vibrational self-relaxation rate constants<sup>22,26,30</sup>, *i.e.* smaller than  $1 - 4 \times 10^{-12} \text{ cm}^3 \text{ molecule}^{-1} \text{ s}^{-1}$  for the levels 7 – 16 explicitly considered in the quantitative analyses discussed later. We note that  $k_{V,v'}[\text{NO}]$  (the slow decay rate of the signals at long times in Figures 2 and 3) is very small in comparison with the two other rates involving formation of level  $v'$ , and we neglect the additional formation of population in level  $v'$  by this process. We may see qualitatively the physical significance of the time dependence in equation (2) if we set  $k_{V,v'}[\text{NO}]$  to zero; the signal then comprises two exponential rises, the rates of which are controlled by two processes  $k_A$  (fast) and  $k_{aX}[\text{NO}]$  (slow). In the Appendix we show how  $B$  and  $C$  will change with  $[\text{NO}]$ , and note that the measurement of the ratio  $B/C$  rather than absolute values will eliminate any inaccuracies caused by the signal normalisation method described earlier. We also show in the Appendix that the ratio  $B/C$  is given closely (to within a few percent) by  $\alpha_{v'}$ , where

$$\frac{B}{C} \approx \alpha_{v'} = \frac{k_{AX}[\text{NO}]\Phi_{AX}^{v'} + k_F\Phi_F^{v'}}{k_{Aa}[\text{NO}]\Phi_{aX}^{v'}} = \beta_{v'} + \frac{k_F\Phi_F^{v'}}{k_{Aa}[\text{NO}]\Phi_{aX}^{v'}} \quad (3)$$

$\alpha_{v'}$  can be seen to be the ratio of the yields of NO  $X(v')$  from the fast (direct quenching from  $A - X$  plus fluorescence) to slow (indirect quenching via  $A - a - X$ ) processes, and  $\beta_{v'}$  is the ratio that we seek, the yields of NO  $(v')$  from the direct and indirect collisional quenching processes. We may now see qualitatively how the signals observed in the early and late time spectra in Figure 1 relate to the rate constants and quantum yields. As an example, we take the data corresponding to emission from  $v' = 13$  near  $3100 \text{ cm}^{-1}$ . The ratio of the early time to late time signals is approximately unity, and if we take this ratio to be equal to  $B/C$  and hence to  $\alpha_{v'}$ , it is clear that for  $v' = 13$  the indirect process (quenching *via* the  $a$  state) is as important as direct formation of the ground state. This simple analysis is an approximation, as the early time signal in Figure 1 has some contribution from the slow process, and (to a smaller extent) the additional late time signal will be reduced by vibrational relaxation. Furthermore, the intensities at a given wavenumber have contributions from other vibrational levels – for example the peak at  $3075 \text{ cm}^{-1}$  is composed of the P branch of the  $(13, 11)$  transition and the R branch of the  $(14, 12)$  transition. However, the result agrees with the intuitively satisfactory premise that the fast/slow ratio of signals indicate the relative proportions by which levels  $v'$  are formed from direct ( $A - X$ ) and indirect ( $A - a - X$ ) processes.

We now consider the filter data, and the filter characteristics are summarised in Table 1. The model was fitted to the observed time dependences (such as the data presented in Figures 2 and 3), accounting for the instrument response function as described above, to yield the rate constants  $k_{aX}$  and  $k_{V,v'}$  together with the coefficients  $A$ ,  $B$  and  $C$  which are now average values for each filter, and which we consider in the next section. The values of  $k_A$  were constrained to those as calculated above.  $k_{V,v'}$  was not well determined over the time scales shown in the Figures, but was of the order of  $5 \times 10^{-13} \text{ cm}^3 \text{ molecule}^{-1} \text{ s}^{-1}$  as expected. The fits are shown as solid lines in Figures 2 and 3. In figure 2a (where no slow rise is observed) we show an expanded version of the signal rise time, showing that the fitting routine captures the unavoidable ringing of the detector. Although the fits seem precise, it was found that the fitting parameters depended closely on the assumed form of the detector response, and the lowest uncertainties occurred when the amplitude of the slow rising contribution was at its largest compared with that of the fast rising component: Figure 2 shows that this condition is best met by filters d) and e). From equation 2 we expect the slow rising term to depend exponentially upon  $k_{aX}[\text{NO}]$ , and Figure 5 shows that this is the case with a plot of the rising rates for filters d) and e) being a linear function of  $[\text{NO}]$  and passing within experimental error through the origin, and with the slope the same for each filter, *i.e.* for each set of vibrational levels probed, between  $v' = 11$  and 16. For filter c) the slow rising rates were less well determined, and were consistently below the straight line fit values for filters

d) and e) by some 10% at 100 mTorr, rising to 20% at 40 mTorr, Filter c) shows a higher ratio of fast to slow contributions than for filters d) and e), and this is believed to be the reason for the deviations, particularly at low NO pressures. For filters b) and f) the fitting process was again less robust because the vibrational relaxation term  $k_{V,v'}$  maximised and the magnitude of the slow increase in signal minimised. From Figure 5 we identify  $k_{aX} = (8.80 \pm 1.1) \times 10^{-11} \text{ cm}^3 \text{ molecule}^{-1} \text{ s}^{-1}$  as the rate constant for the rate determining step in the formation of  $\text{NO X } ^2\Pi$  ( $v = 11 - 16$ ) from the levels of  $\text{NO a } ^4\Pi$  produced by collisional self-quenching of  $\text{NO A}^2\Sigma^+$  ( $v = 0$ ) where the error quoted is two standard deviations in the slope of a straight line fitted to the weighted values of the points. The rate determining step could be either vibrational self-relaxation of the initially formed levels of  $\text{NO a } ^4\Pi$  or intersystem crossing from a  $^4\Pi$  into  $X^2\Pi$ , and we cannot formally attribute the measured process to either of these (or a combination of them). The rate constant is high, almost gas kinetic, and would be very large for a vibrational relaxation process, particularly because the energy discrepancy between the vibrational quanta of the  $\text{NO(a)}$  and  $\text{NO(X)}$  states would suggest that single vibrational quantum energy transfer would be inefficient, but two quanta loss in  $\text{NO(a)}$  would be close to resonance with a single quantum gain in  $\text{NO(X)}$ . We see that the rate constant is independent of the final vibrational level reached in  $\text{NO X } ^2\Pi$  for the two filters analysed. This would be consistent with either the formation of a single vibrational level of the  $^4\Pi$  state (as we have assumed in the analysis), or that the energy level(s) produced all relax to the observed vibrationally excited ground state levels with the same collisional rate constant.

#### D. Kinetic analysis - Quantum yields

Figures 1, 2 and 3 show that the slow process, which we attribute to  $\text{NO(X, } v')$  formed by collisional quenching of the a state, is clearly observed to take place for vibrational levels  $v' = 5$  and above, with levels around  $v' = 11$  and 12 showing the largest increase, such that the emission intensity from levels formed in this slow process is approximately equal to that from the fast process. In principle an analysis of the vibrational level populations from time resolved spectra such as in Figure 1 can reveal the relative contributions from the slow and fast processes. In practice however there are two problems which did not occur when this approach was used to determine the total collisional quenching population distribution in our earlier work.<sup>15</sup> First, the fast HgCdTe detector is noisier than the slower InSb detector used previously which adds to uncertainties in the derived populations. Secondly, we are forced to operate under conditions where fluorescence from the A state rather than its collisional quenching dominates. Working at higher pressures as used previously<sup>15</sup> results in the separation of fast and slow rising signals becoming impossible to untangle because of the detector rise time. The problem is particularly acute for the formation of low vibrational levels where although the total vibrational populations from quenching are highest, fluorescence dominates - at 100 mTorr pressure of NO the

fractional yields from fluorescence are  $> 85\%$  for vibrational levels  $v' = 4$  and below. What follows are approximate values that we can obtain on the relative magnitudes of the fast and slow quenching contributions from the filter experiments.

We first deal with the data from filters d) and e). Formation of NO(X) in these levels ( $v' = 11 - 13$  and  $13 - 16$ ) by fluorescence can be neglected: we may calculate from the previously measured total (fast plus slow) quenching quantum yields<sup>15</sup> plus the fluorescence quantum yields obtained from the Einstein A coefficients (recently calculated for transitions up to the highest vibrational levels in the X state observed in the present experiments<sup>35</sup>) that for filters d) and e) the A – X fluorescence contribution to the total populations observed is  $< 3\%$  and  $< 1\%$  respectively. Measured values of  $B/C$  are given in Table 1: for the best S/N ratio data, filter e), they show very little variation with [NO], with a standard deviation of  $3\%$ , rising to  $8\%$  for the noisier data of filter d). This is what is expected in equation (3) when we set  $\Phi_F^{v'} = 0$ , and hence  $\alpha_{v'} = \beta_{v'}$ . We note however that we do not have data for a single vibrational level  $v'$ , but rather for a range passed by each filter. For the widest bandwidth (filter e)) the radiation transmitted is approximately  $15\%$  from  $v' = 13$ ,  $45\%$  from  $v' = 14$  and  $40\%$  from  $v' = 15$ . We note in passing that the emission data will always have contributions from at least two vibrational levels because of the nature of the constructive overlap of the overtone transitions, and this problem will not be solved by the use of narrower band filters. We thus can only calculate an average ratio of  $\beta$  in Equation 3 from the  $B/C$  values which will strictly only be valid if the ratio  $\frac{\Phi_{AX}^{v'}}{\Phi_{aX}^{v'}}$  remains invariant over the range of levels passed by the filter. It can be seen from Figure 1 that the fast/slow ratio is not changing abruptly over this narrow wavenumber range and an average value will be meaningful when we consider the approximate nature of our calculation of quantum yields. The data are shown in Table 1 as values of  $\bar{\beta}$ , (in these three cases equal to the average value of the parameter  $\alpha$ , which we call  $\bar{\alpha}$ ), then converted into average values of  $\bar{\gamma}$ , the quantum yield of the formation of NO(a) from the collisional quenching of NO(A) over the vibrational levels transmitted by the filter, where  $\bar{\gamma} = (\bar{\beta} + 1)^{-1}$ . We see that for filters d) and e)  $\bar{\gamma} = 0.6$  and  $0.5$  respectively, showing that approximately half the vibrational levels between 11 and 16 are formed via the a state. For the single data point for filter f) we find  $\bar{\gamma} = 0.3$ , *ie.* direct quenching to these high levels dominates.

For vibrational levels below  $v' = 11$  we cannot ignore their formation by A – X fluorescence. Equation 3 shows that for a given vibrational level  $v'$  a plot of  $\alpha_{v'}$  against  $1/[\text{NO}]$  should be a straight line with intercept  $\beta_{v'}$ , but we must again recognise that we are not dealing with a single level  $v'$  but contributions from several levels. For filter c) for example, the contribution is approximately half from level 7 and half from level 8, and thus the values of the three quantum yields  $\Phi^{v'}$  in equation 3 need to be replaced by summations over the fractional contributions  $f_{v'}$  from the vibrational levels  $v'$ , *ie.*  $\sum_{v'} f_{v'} \Phi^{v'}$ . Figure 6 shows a plot of  $\bar{\alpha}$  against  $1/[\text{NO}]$  to be accurately represented by a straight line

for NO pressures between 30 and 100 mTorr, a range over which the fluorescence contribution to the population decreases from 54 to 29%. From the intercept of the plot (see equation (3)) we retrieve a value of  $\bar{\beta} = 1.03 \pm 0.06$  and  $\bar{\gamma} = 0.5$ .

**Table 1**

Filter	a	b	c	d	e	f
Central Peak/cm <sup>-1</sup>	3680	3486	3396	3160	3033	2750
Bandwidth/cm <sup>-1</sup>	125	83	70	67	143	125
$\nu'$ range	2 – 4	5 – 7	7 – 9	11 – 13	13 – 16	17 – 20
[NO]/mTorr	20 – 100	50	30 – 100	40 – 100	20 – 100	50
$B/C$	-	3.14	2.21 – 1.37	$0.65 \pm 0.16$	$0.90 \pm 0.1$	2.05
% fluorescence	98 – 90%	69%	54 – 29%	3 – 1.3%	0.8 – 0.2%	<.01%
$\bar{\beta} = \left(\frac{Fast}{Slow}\right)_{Coll}$	-	-	$1.03 \pm 0.06$	$0.65 \pm 0.1$	$0.96 \pm 0.06$	2.1
$\bar{\gamma}$	0	0	0.49	0.61	0.51	0.32

**Table 1.** Data for the filter experiments. For the six filters used the first three rows give the central peaks (also shown in Figure 1), the bandwidths, and the vibrational levels  $\nu'$  in NO X <sup>2</sup>Π observed in first overtone transitions through them. The fourth row shows the range of NO pressures used for the evaluation of the ratios  $B/C$  with the values given in the fifth row. For filters d) and e) the averages are given over the pressure range with 2σ error bars: for filter c) the values change as a function of NO pressure as explained in the text, and are calculated from the plot of Figure 6. The sixth row shows the contribution to the signal passed through the filter from NO X <sup>2</sup>Π  $\nu'$  levels formed by fluorescence from NO A <sup>2</sup>Σ<sup>+</sup> ( $\nu = 0$ ). The final rows shows the values of  $\bar{\beta}$ , the average ratio of the populations of the vibrational levels appropriate to filters c) – f) formed by fast and slow collisional processes, and  $\bar{\gamma}$  the quantum yields of NO( $\nu'$ ) formed collisionally by self-quenching of the A state through the indirect and slow process A – a – X.

For filter b) although it can be seen from Figures 1 and 2 that there is a contribution from slow quenching, the fractional population produced by fluorescence at 50 mTorr (Figure 2) is now 69%. The observed value of  $B/C$ , 3.14, can be converted to a value of  $\bar{\beta} = 0.29$  by the algebraic manipulations used for the other filters, but the potential errors are large, as we are effectively subtracting two similar numbers – an error of 10% in  $B/C$  translates to an error of 35% in  $\bar{\beta}$ . We therefore simply note that there is a contribution from the slow process, but make no quantitative estimate of it. For filter a) (where the emission produced by fluorescence is between 90 – 98% of the total) we are unable to discern a slow

component, but this may be masked by the relatively fast contribution from vibrational quenching. For these filters (and for all levels produced in  $v' < 7$ ) we set  $\bar{\gamma} = 0$ .

The data are summarised in Table 1, and we now attempt to make an estimate of the quantum yields for collisional quenching which leads to the X and the a states. We have data on  $\bar{\gamma}$  for levels 7 – 9, 11 – 13, 13 – 16 and 17 – 19. We first assume that the values of  $\bar{\gamma}$  for the missing levels (around  $v' = 10$ ) is the average for the sets of levels on either side measured with filters c) and d). The spectral data shown in Figure 1 shows that this assumption is reasonable. We then combine the fractional total populations in these levels<sup>15</sup> ( $v' = 7$  and above) with the values of  $\bar{\gamma}$  to obtain an overall population weighted value of the quantum yield of a  $^4\Pi$  state formation. The value is 0.51 indicating the slow collisional process accounts for formation of about half of the total collisional population of these levels. The levels  $v' \geq 7$  account for 37% of the total collisionally formed states<sup>15</sup>. For levels below  $v' = 7$  we know that there is slow formation from the evidence of the spectra and of data for filter b), but we are unable to make a quantitative estimate of it: we set the contribution of the slow process to zero for these levels, and thus make a lower limit of the overall quantum yield  $k_{Aa}/(k_{Aa} + k_{AX})$  as being  $0.37 \times 0.51 = 0.19$  or 19%.

We place several caveats on this estimate. It relies upon the populations in  $v' = 7$  and above being 37% of the total population from A state quenching. Populations were taken from previous measurements in our group<sup>15</sup>, which used surprisal analysis of the higher  $v'$  populations ( $v' = 2 - 20$ ) to estimate those in the unobserved  $v' = 0$  and 1 levels, and the analysis assumed a single surprisal parameter. If there are two distributions of levels with different surprisal parameters for the populations produced from fast and slow quenching then such an extrapolation could be in error. For it to reduce the estimate of 19% quenching to the a  $^4\Pi$  state however it would need to show a marked increase in the unobserved populations ( $v' = 0$  and 1) produced by direct A – X quenching, and the surprisal analysis for the total quenching populations shows no indication of this for any observed low  $v'$  levels.<sup>15</sup> We also assume that our measured filter data can be converted into quantum yields by assuming that for a given filter there is no variation of quantum yield ratios with  $v'$  over the levels transmitted. Despite these caveats, we conclude that the collisional self-quenching of the A state produces a non-negligible population in the a  $^4\Pi$  state, particularly for vibrational levels  $\geq 7$ .

## Discussion

Self-quenching of NO A  $^2\Sigma^+$  ( $v = 0$ ) is fast at room temperature,<sup>25, 35-43</sup> with the most recent value<sup>25</sup> being measured as  $(2.71 \pm 0.06) \times 10^{-10} \text{ cm}^3 \text{ molecule}^{-1} \text{ s}^{-1}$ . The cross section increases as the temperature is lowered from 294 K<sup>25,43,44</sup> and shock tube studies have indicated a small increase at considerably

higher temperatures.<sup>45,46</sup> This evidence has been used to suggest a complex forming mechanism reliant on dispersive forces<sup>25,42</sup> rather than a harpoon type mechanism.<sup>47</sup> Complex formation would be expected to give an approximately statistical distribution of quenched molecules in the X state, rather than a distribution dominated by low vibrational levels which would be more characteristic of Franck Condon (FC) factors connecting the NO<sup>+</sup> ion and the ground NO(X) state in a harpoon mechanism. The former outcome is closer to that observed in the total vibrational level distribution of NO(X), where a slightly hotter than statistical population distribution was observed,<sup>15</sup> but we must now recognise that two distributions are involved. We note that if FC factors for the a – X transition control the final state distribution in NO(X) produced by quenching of the a <sup>4</sup>Π state then we would expect the dominance of high vibrational levels because of the markedly different equilibrium internuclear separations in the two states. For example, for a <sup>4</sup>Π (ν = 0) the FC factors peak for the transition terminating on ν' = 9 in the ground state.<sup>2</sup> If this is so we would expect a low contribution from low vibrational levels, and our estimate of 19% for the fraction of A state molecules being quenched to the a state would appear to be a reasonable one. On the other hand if a distribution closer to statistical were taking place then we would expect the quantum yields of low vibrational levels to be considerable, and 19% would be very much a lower estimate.

The formation of both the X and a states by self-quenching of NO A <sup>2</sup>Σ<sup>+</sup> is spin allowed, as is the process that we identify as self-quenching of the a <sup>4</sup>Π state, and the rate constants for all processes are fast. Our measured a – X collisional self-quenching rate constant ( $8.80 \times 10^{-11} \text{ cm}^3 \text{ molecule}^{-1} \text{ s}^{-1}$ ) is close to that measured for the loss of NO a <sup>4</sup>Π (ν = 11) to nearby B <sup>2</sup>Π vibrational levels ( $14 \times 10^{-11} \text{ cm}^3 \text{ molecule}^{-1} \text{ s}^{-1}$ )<sup>9,11</sup> but is a factor of 7 faster than that inferred from the cross section measurements of Ottinger and Shen<sup>12</sup> for the reverse process in equation 1 (corresponding to a thermal rate constant of  $1.3 \times 10^{-11} \text{ cm}^3 \text{ molecule}^{-1} \text{ s}^{-1}$ ). The latter authors however stress their value depends crucially upon the assumed vibrational population distribution in the ν ≥ 6 levels of the a <sup>4</sup>Π state in their experiment and may be subject to considerable errors. We note that the participation of the a <sup>4</sup>Π state in the quenching of NO A <sup>2</sup>Σ<sup>+</sup> (ν = 0) has been postulated,<sup>48</sup> but only for slow quenchers which show a positive increase in cross section with increasing temperature, and suggested as being caused by a curve crossing between the A <sup>2</sup>Σ<sup>+</sup> and a <sup>4</sup>Π states above the zero point energy of the A <sup>2</sup>Σ<sup>+</sup> state. This model cannot apply to the very rapid self-quenching observed here. Involvement of the a <sup>4</sup>Π state has been suggested as a possibility leading to the formation of HNO following excitation of NO/H<sub>2</sub> mixtures.<sup>49</sup>

Is the a <sup>4</sup>Π state important in combustion and aeronomy processes? So far we have only demonstrated its participation in the self-quenching of NO A <sup>2</sup>Σ<sup>+</sup> by ground state NO, which would be of minor interest in these areas, particularly because quenching by ground state oxygen will dominate. However if formation of the a <sup>4</sup>Π state is efficient in other spin allowed processes, then collisions with O<sub>2</sub> <sup>3</sup>Σ<sub>g</sub><sup>-</sup> need to be considered. We have looked at the dynamics of formation of high vibrational levels

of NO X ( $v'$ ) from the quenching of NO(A) in the presence of O<sub>2</sub>,<sup>16</sup> and have made preliminary studies which show both fast and slow components of the emission of ground state overtone transitions, but the system is complicated by their potential formation from four processes (direct and indirect quenching by both NO and O<sub>2</sub>) and also because the vibrational relaxation of NO( $v'$ ) with O<sub>2</sub>, which peaks at  $v'=13$ , is faster than the comparable process with NO near this vibrational level.<sup>50</sup> However, what we have found unexpectedly is that Xe may act as a convenient *marker* for NO a <sup>4</sup>Π production. In the presence of Xe we observe a large increase in emission from highly vibrationally excited levels of NO(X,  $v'=10-20$ ). Xe does not quench the NO(A) state efficiently (the rate constant is  $\leq 1.6 \times 10^{-14}$  cm<sup>3</sup> molecule<sup>-1</sup> s<sup>-1</sup>)<sup>24</sup> but appears to produce these levels by quenching of NO a <sup>4</sup>Π in an indirect mechanism similar to (but slower by a factor of 30 than) that for NO described above. The nature of this spin forbidden mechanism is not clear, but may be a consequence of the large spin orbit interaction in ground state Xe which facilitates coupling between Xe and the a<sup>4</sup>Π state ( $\Lambda = 1$ ) but not the A <sup>2</sup>Σ<sup>+</sup> state ( $\Lambda = 0$ ). Conditions can be found where the indirect (slow) NO (X,  $v'$ ) formation is dominated by Xe collisions, and thus any change in the a <sup>4</sup>Π state quantum yield (such as might occur in collisions with O<sub>2</sub>) should be manifest in the yield of high vibrational states by the indirect process. If this hypothesis proves to be correct, then measurement of the high vibrational levels should result in quantitative estimation of the quantum yields of NO a <sup>4</sup>Π, as they will be free from any fluorescence contributions which result in the present quantum yield estimates being lower limits. Such experiments will be carried out in future when circumstances permit.

## Conclusions

Vibrationally excited NO X <sup>2</sup>Π ( $v'$ ), formed following collisional quenching of NO A <sup>2</sup>Σ<sup>+</sup> ( $v=0$ ) by NO X <sup>2</sup>Π ( $v'=0$ ) is produced on two time scales. The first is a fast production rate (*ca.* 200 ns) the time scale of which is consistent with direct quenching of NO A <sup>2</sup>Σ<sup>+</sup> ( $v=0$ ) and controlled by the radiative decay rate which dominates at the low pressures of NO ( $\leq 100$  mTorr) used. A second slower process is seen, populating some of the same vibrational levels at rates which are pressure dependent. A reservoir state formed by quenching of NO A <sup>2</sup>Σ<sup>+</sup> ( $v=0$ ) is invoked to explain the observations, and the available evidence points to this state being the first electronically excited state of NO, a <sup>4</sup>Π, formed in a spin allowed process in collisions with ground state NO. The quantum yield for formation of NO a <sup>4</sup>Π formed by collisional quenching of NO A <sup>2</sup>Σ<sup>+</sup> ( $v=0$ ) by NO is estimated to be at least 19% , and the rate constant for quenching of the NO a <sup>4</sup>Π state by NO (again a spin allowed process) is measured as  $(8.80 \pm 1.1) \times 10^{-11}$  cm<sup>3</sup> molecule<sup>-1</sup> s<sup>-1</sup> at 298 K. Future experiments designed to see if similar spin allowed processes occur in collisions with molecular oxygen are discussed, particularly as they may be of importance in combustion and aeronomy processes.

## Conflicts of interest

There are no conflicts to declare.

## Acknowledgements

We are grateful to the EPSRC for financial support through Grant EP/L025833/1 “Infrared emission from the quenching of electronically excited states”. L.L. is grateful to the Royal Society of Chemistry for the award of a Researcher Mobility Grant.

## References

- 1 C. Ottinger and A. F. Vilesov, *J. Chem. Phys.*, 1994, **100**, 1815–1822.
- 2 M. Drabbels, C. G. Morgan and A. M. Wodtke, *J. Chem. Phys.*, 1995, **103**, 7700–7707.
- 3 R. A. Young and R. L. Sharpless, *Discuss. Faraday Soc.*, 1962, **33**, 228–256.
- 4 R. A. Young and R. L. Sharpless, *J. Chem. Phys.*, 1963, **39**, 1071–1102.
- 5 I. M. Campbell and R. S. Mason, *J. Photochem.*, 1978, **8**, 321–336.
- 6 I. M. Campbell and B. A. Thrush, *Proc. R. Soc. A Math. Phys. Eng. Sci.*, 1967, **296**, 201–221.
- 7 C. Ottinger and A. F. Vilesov, *J. Chem. Phys.*, 1994, **100**, 1805–1814.
- 8 P. C. Cosby, R. A. Copeland, D. G. Williamson, G. Gaudin, M. J. Dyer, D. L. Huestis and T. G. Slinger, *J. Chem. Phys.*, 1997, **107**, 2249–2256.
- 9 R. A. Copeland, M. J. Dyer, D. L. Huestis and T. G. Slinger, *Chem. Phys. Lett.*, 1995, **236**, 350–354.
- 10 R. A. Copeland, M. J. Dyer, H. I. Bloemink and T. G. Slinger, *J. Chem. Phys.*, 1997, **107**, 2257–2266.
- 11 R. A. Copeland, M. J. Dyer and T. G. Slinger, *Chem. Phys. Lett.*, 1995, **241**, 173–179.
- 12 C. Ottinger and G. Shen, *Chem. Phys. Lett.*, 1998, **289**, 231–240.
- 13 K.-P. Huber and G. Herzberg, *Molecular spectra and molecular structure. IV, Constants of diatomic molecules*, .
- 14 T. B. Settersten, B. D. Patterson, H. Kronmayer, V. Sick, C. Schulz and J. W. Daily, *Phys. Chem. Chem. Phys.*, 2006, **8**, 5328–5338.

- 15 G. Hancock and M. Saunders, *Phys. Chem. Chem. Phys.*, 2008, **10**, 2014–2019.
- 16 M. A. Burgos Paci, J. Few, S. Gowrie and G. Hancock, *Phys. Chem. Chem. Phys.*, 2013, **15**, 2554–2564.
- 17 J. Few, J. D. Fletcher, G. Hancock, J. L. Redmond and G. A. D. Ritchie, *Phys. Chem. Chem. Phys.*, 2017, **19**, 11289–11298.
- 18 P. C. Cosby, D. L. Huestis and T. G. Slanger, *J. Chem. Phys.*, 1992, **97**, 5952–5955.
- 19 T. B. Settersten, B. D. Patterson and W.H. Humphries, *J. Chem. Phys.*, 2009, **131**, 104309.
- 20 G. Hancock and V. Haverd, *Phys. Chem. Chem. Phys.*, 2003, **5**, 2369–2375.
- 21 G. Hancock and M. Morrison, *Mol. Phys.*, 2005, **103**, 1727–1733.
- 22 G. Hancock, M. Morrison and M. Saunders, *Phys. Chem. Chem. Phys.*, 2009, **11**, 8507–8515.
- 23 H. L. Welsh, C. Cumming and E. J. Stansbury, *J. Opt. Soc. Am.*, 1951, **41**, 712–714.
- 24 J. Few and G. Hancock, *Phys. Chem. Chem. Phys.*, 2014, **16**, 11047–11053.
- 25 T. B. Settersten, B. D. Patterson and C. D. Carter, *J. Chem. Phys.*, 2009, **130**, 204302.
- 26 H. Horiguchi and S. Tsuchiya, *Jpn. J. Appl. Phys.*, 1979, **18**, 1207–1211.
- 27 M. Islam, I. W. M. Smith and J. W. Wiebrecht, *J. Phys. Chem.*, 1994, **98**, 9285–9290.
- 28 I. J. Wysong, *J. Chem. Phys.*, 1994, **101**, 2800–2810.
- 29 J. A. Dodd, R. B. Lockwood, S. M. Miller and W. A. M. Blumberg, *J. Chem. Soc., Faraday Trans.*, 1997, **93**, 2637–2644.
- 30 X. Yang, E. H. Kim and A. M. Wodtke, *J. Chem. Phys.*, 1992, **96**, 5111–5122.
- 31 D.C. Jacobs, R.J. Madix and R.N. Zare, *J. Chem. Phys.*, 1986, **85**, 5469 – 5479.
- 32 H. Zacharias, F. de Rougemont, T.F. Heinz and M.M.T. Loy, *J. Chem. Phys.*, 1996, **105**, 111–117.
- 33 S.R. Langhoff, C.W. Bauschlicher Jr and H. Partridge, *Chem. Phys. Lett.*, 1994, **223**, 416–422
- 34 H. Lefebvre-Brion and F. Guerin, *J. Chem. Phys.* 1968, **49**, 1446–1447.
- 35 J. Cheng, H. Zhang, X. Cheng and X. Song, *Mol. Phys.*, 2017, **115**, 2577–2585.36 I. S. McDermid and J. B. Laudenslager, *J. Quant. Spectrosc. Radiat. Transf.*, 1982, **27**, 483–492.

- 37 M. Asscher and Y. Haas, *J. Chem. Phys.*, 1982, **76**, 2115–2126.
- 38 Y. Haas and G. D. Greenblatt, *J. Phys. Chem.*, 1986, **90**, 513–517.
- 39 G. D. Greenblatt and A. R. Ravishankara, *Chem. Phys. Lett.*, 1987, **136**, 501–505.
- 40 G. A. Raiche and D. R. Crosley, *J. Chem. Phys.*, 1990, **92**, 5211–5217.
- 41 J. B. Nee, C. Y. Juan, J. Y. Hsu, J. C. Yang and W. J. Chen, *Chem. Phys.*, 2004, **300**, 85–92.
- 42 R. Zhang and D. R. Crosley, *J. Chem. Phys.*, 1995, **102**, 7418–7424.
- 43 T. B. Settersten, B. D. Patterson and J. A. Gray, *J. Chem. Phys.*, 2006, **124**, 234308.
- 44 R. Sánchez-González, R. D. W. Bowersox and S. W. North, *Opt. Lett.*, 2014, **39**, 2771–2774.
- 45 P. H. Paul, J. A. Gray, J. L. Durant and J. W. Thoman, *Chem. Phys. Lett.*, 1996, **259**, 508–514.
- 46 J. A. Gray, P. H. Paul and J. L. Durant, *Chem. Phys. Lett.*, 1992, **190**, 266–270.
- 47 P. H. Paul, J. A. Ray, J. L. Durant and J. W. Thoman, *AIAA J.*, 1994, **32**, 1670–1675.
- 48 M. C. Drake and J. W. Ratcliffe, *J. Chem. Phys.*, 1993, **98**, 3850–3865.
- 49 A. B. Callear and P. M. Wood, *Trans. Faraday Soc.*, 1971, **67**, 3399–3406.
- 50 G. Hancock, M. Morrison and M. Saunders, *Chem. Phys. Lett.* 2006, **425**, 216–220.

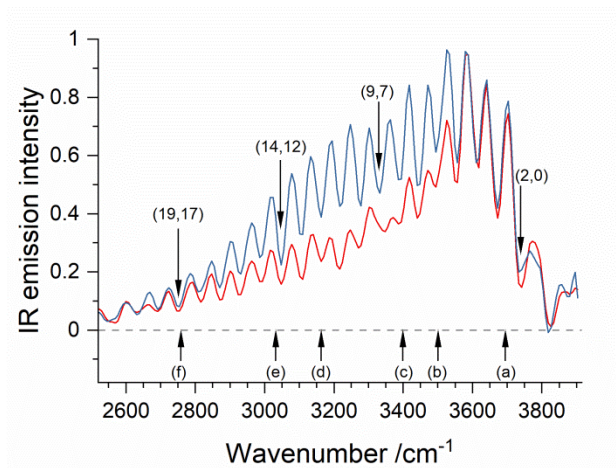


**Figure 1:** The infrared emission resulting from first overtone transitions ( $\Delta v' = -2$ ) within NO X  $^2\Pi(v')$  observed between 0.8 and 1.8  $\mu\text{s}$  (red curve) and 9 – 10  $\mu\text{s}$  (blue curve) following irradiation of 100 mTorr NO to form NO A $^2\Sigma^+(v=0)$ , in the presence of 50 Torr Ar, with selected band origins marked. Central transmission wavenumbers for optical filters a) – f) used in experiments described below are also included.

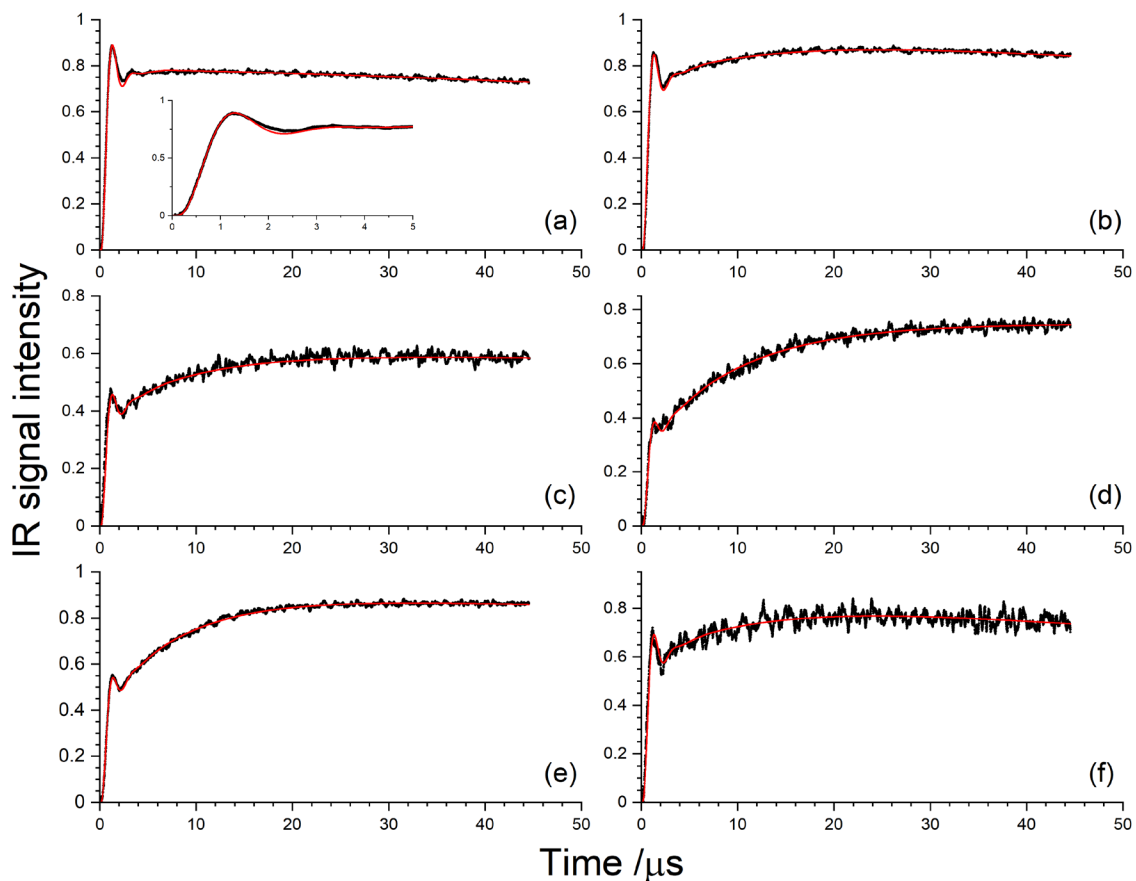


**Figure 2:** The infrared emission transmitted by filters a) – f) resulting from first overtone transitions ( $\Delta v' = -2$ ) within  $\text{NO } X^2\Pi(v')$  following excitation of 50 mTorr NO at 226 nm, in the presence of 8 Torr Ar. Filter characteristics are given in Table 1 and their central wavenumbers shown in Figure 1. Best fits to a triple exponential kinetic model (equation 2 convoluted with the appropriate instrument response function) are also included. An expanded insert in the data for filter a) shows the result of the fitting at early times and the effect of the unavoidable ringing of the signal.

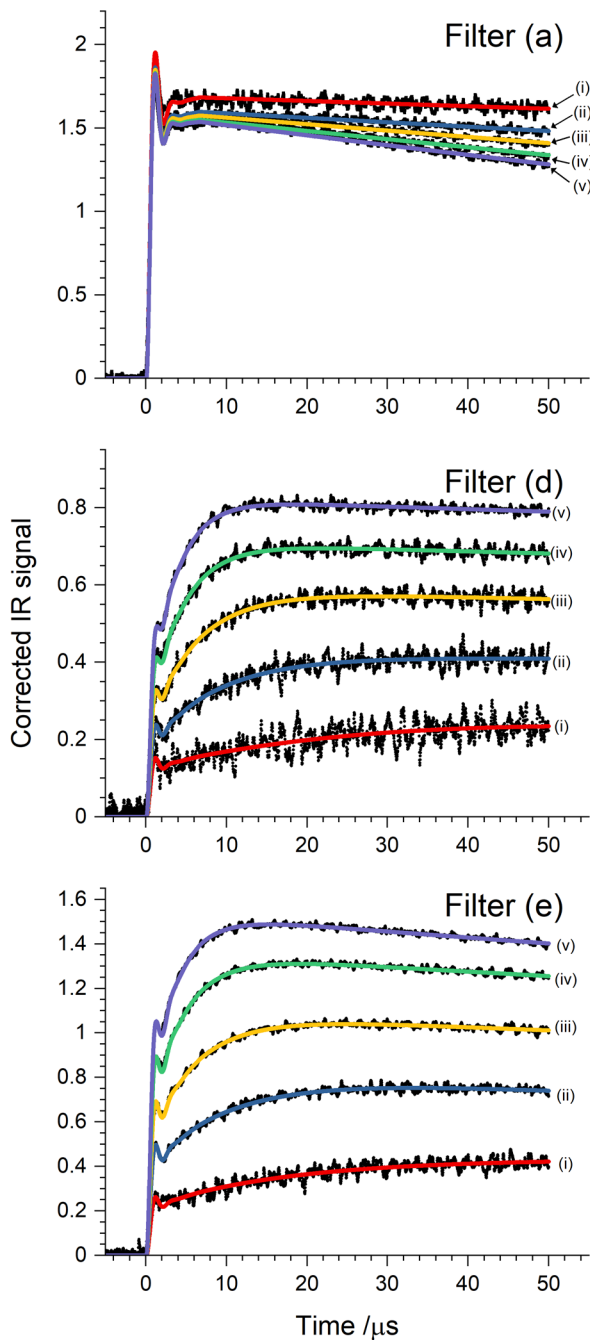


**Figure 3:** IR emission filter traces for regions a), d) and e) (including best fits to the kinetic model, Equation 2) obtained at constant Ar pressure (8 Torr) and NO pressures of i) 20 mTorr (red), ii) 40 mTorr (blue), iii) 60 mTorr (yellow), iv) 80 mTorr (green), and v) 100 mTorr (purple). All data are normalised to the uv fluorescence (*ie.* they represent signals from the same concentrations of NO(A)).

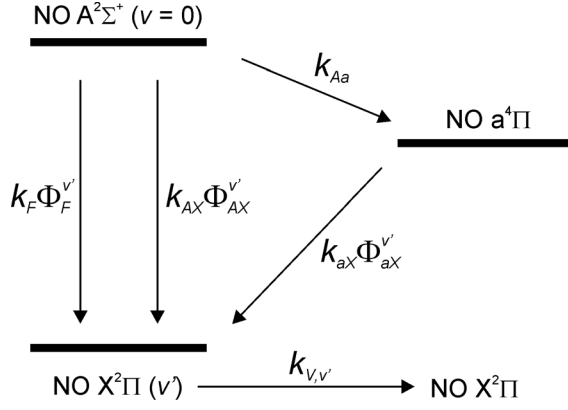


**Figure 4:** Kinetic scheme. In equations and main text we assign a combined pseudo first order rate constant  $k_A$  to all processes responsible for the removal of NO A<sup>2</sup>Σ<sup>+</sup>. We assume initially for the kinetic analysis that one vibrational level  $v$  is produced in NO a<sup>4</sup>Π, and that the total second order loss rate constant for the NO a<sup>4</sup>Π state is given by the sum of the  $k_{aX} \Phi_{aX}^{v'}$  rate constants over all  $v'$ , which we call  $k_{aX}$ .  $k_{v,v'}$  is the net removal rate constant for the vibrational level  $v'$  in collisions with NO,

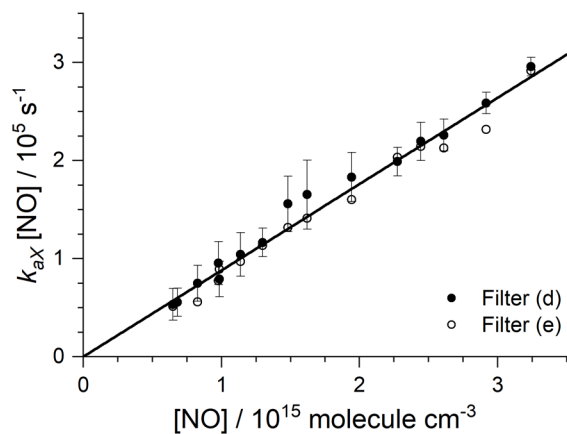


**Figure 5:** Rates of rise of the slow component of IR emission from NO X  $^2\Pi$  ( $\nu'$ ) transmitted by filters d) and e) observed when NO is excited at 226.26 nm and subsequently quenched. Error bars represent one standard deviation from multiple measurements at each NO pressure. Points from filters d) and e) have been combined and the straight line fit yield a rate constant  $k_{aX}$  of  $(8.80 \pm 1.1) \times 10^{-11}$  cm<sup>3</sup> molecule<sup>-1</sup> s<sup>-1</sup>. The error quoted is  $2\sigma$ .

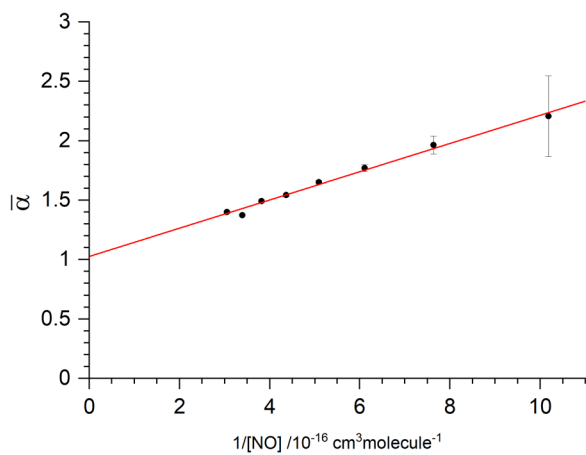


**Figure 6.** Plot of  $\bar{\alpha}$  calculated from the values of  $B/C$  measured for filter c) between 30 and 100 mTorr  $[\text{NO}]$ , plotted as a function of  $1/[\text{NO}]$  as in equation 3. The intercept gives a value of  $\bar{\beta} = 1.03 \pm 0.06$  where the error is  $2\sigma$ .

## Appendix 1 – The Kinetic model

We solve the rate equations for the time dependences of the concentrations of NO in the three electronic states A, a and X. These concentrations are denoted as  $[\text{NO}, \text{A}](t)$ ,  $[\text{NO}, \text{a}](t)$  and  $[\text{NO}, \text{X}, v'](t)$  respectively and the relevant rate equations are:

$$\begin{aligned}\frac{d[\text{NO}, \text{A}]}{dt} &= -k_A[\text{NO}, \text{A}] \\ \frac{d[\text{NO}, \text{a}]}{dt} &= (k_{Aa}[\text{NO}, \text{A}] - k_{aX}[\text{NO}, \text{a}])[\text{NO}] \\ \frac{d[\text{NO}, \text{X}, v']}{dt} &= [k_{AX}[\text{NO}]\Phi_{AX}^{v'} + k_F\Phi_F^{v'}][\text{NO}, \text{A}] + k_{aX}[\text{NO}]\Phi_{aX}^{v'}[\text{NO}, \text{a}] - k_{v,v'}[\text{NO}][\text{NO}, \text{X}, v']\end{aligned}$$

The solution for the time dependence of  $[\text{NO}, \text{X}, v']$  is

$$[\text{NO}, \text{X}, v'](t) = Ae^{-k_{v,v'}[\text{NO}]t} - Be^{-k_A[\text{NO}]t} - Ce^{-k_{aX}[\text{NO}]t}.$$

The coefficients  $A$ ,  $B$  and  $C$  are given by

$$\begin{aligned}B &= [\text{NO}, \text{A}]_0 \left( k_{AX}[\text{NO}]\Phi_{AX}^{v'} + k_F\Phi_F^{v'} - \frac{k_{Aa}[\text{NO}]k_{aX}[\text{NO}]\Phi_{aX}^{v'}}{(k_A - k_{aX}[\text{NO}])} \right) (k_A - k_{v,v'}[\text{NO}])^{-1} \\ C &= \frac{[\text{NO}, \text{A}]_0 k_{Aa}[\text{NO}]k_{aX}[\text{NO}]\Phi_{aX}^{v'}}{(k_A - k_{aX}[\text{NO}]) (k_{aX}[\text{NO}] - k_{v,v'}[\text{NO}])} \\ A &= B + C\end{aligned}$$

where the quantum yields,  $\Phi_i^{v'}$ , are as defined in equation (3) in the main text. The ratio  $B/C$  becomes

$$\begin{aligned}\frac{B}{C} &= \left( \frac{k_{AX}[\text{NO}]\Phi_{AX}^{v'} + k_F\Phi_F^{v'}}{k_{Aa}[\text{NO}]\Phi_{aX}^{v'}} \left[ 1 - \frac{k_{aX}[\text{NO}]}{k_A} \right] - \frac{k_{aX}[\text{NO}]}{k_A} \right) \left( \frac{1 - \frac{k_{v,v'}}{k_{aX}}}{1 - \frac{k_{v,v'}[\text{NO}]}{k_A}} \right) \\ &= \left( \alpha_{v'} \left[ 1 - \frac{k_{aX}[\text{NO}]}{k_A} \right] - \frac{k_{aX}[\text{NO}]}{k_A} \right) \left( \frac{1 - \frac{k_{v,v'}}{k_{aX}}}{1 - \frac{k_{v,v'}[\text{NO}]}{k_A}} \right)\end{aligned}$$

From the measured values of  $k_{v,v'}$  and  $k_{aX}$  together with literature values of  $k_A$  the measured ratios  $B/C$  can be converted into values of  $\alpha_{v'}$ . The ratios  $\frac{k_{v,v'}}{k_{aX}}$  and  $\frac{k_{v,v'}[\text{NO}]}{k_A}$  are  $\ll 1$ , and the terms involving  $\frac{k_{aX}[\text{NO}]}{k_A}$  are small corrections, so that  $\frac{B}{C} \approx \alpha_{v'}$ .